RSC Advances

PAPER

Check for updates

Cite this: *RSC Adv.*, 2019, **9**, 30125

Design of GO–Ag-functionalized Fe_3O_4@CS composite for magnetic adsorption of rhodamine B

Lili Xu,[a] Hongbo Suo,[a] Renmin Liu,[a] Houmei Liu*[b] and Hongdeng Qiu*[c]

Received 28th June 2019
Accepted 16th September 2019

DOI: 10.1039/c9ra04897a

rsc.li/rsc-advances

In this study, a novel magnetic composite (Fe_3O_4@CS/GO/Ag) modified with chitosan (CS), graphene oxide (GO) and Ag nanoparticles (Ag NPs) was successfully prepared as an efficient adsorbent for detection of rhodamine B (RB) combined with a fluorescence technique. The properties of the magnetic composite were confirmed by field emission scanning electron microscopy, energy dispersive X-ray spectroscopy, and vibrating sample magnetometry. The components of Fe_3O_4@CS/GO/Ag endowed it with excellent extraction performance and convenient operation. The main parameters affecting extraction and desorption efficiency were all investigated systematically. Under the optimized experimental conditions, the proposed method showed linear ranges (0.2–6.0 μg L^{-1}) with $R^2 = 0.9992$. The limits of detection (LODs) and quantification (LOQs) were 0.05 and 0.2 μg L^{-1} ($n = 3$), respectively. Fe_3O_4@CS/GO/Ag exhibited outstanding extraction efficiency for RB, compared with CS-coated Fe_3O_4 nanoparticles (Fe_3O_4@CS) and GO-modified Fe_3O_4@CS (Fe_3O_4@CS/GO). The applicability of the proposed method was investigated by analyzing four real samples (waste water, soft drink, shampoo, and red pencil) and the spiked recoveries ranged between 94% and 97% with RSD ranging from 3% to 6%, which showed that the proposed method had satisfactory practicability and operability.

1 Introduction

As a synthetic dye, rhodamine B (RB) was initially used as a color additive in textiles, foodstuffs and fluorescent labeling.[1,2] Afterwards, it was widely applied as a colorant in the cosmetic, pharmaceutical, plastic, leather, dyeing, paper and printing industries, resulting in large amounts of wastewater every year.[3,4] Meanwhile, RB is harmful if swallowed by human beings and animals which can cause irritation to the skin, eyes and respiratory tract.[5,6] Furthermore, RB has been found to cause cancer in rats and mice through multiple tests.[7] Because of its hazardous nature and harmful effects, the development of a simple method for the determination of RB in different samples is necessary. Various techniques have been developed for the determination of RB to date, including ultraviolet spectrophotometry,[8–10] capillary chromatography,[11,12] high performance liquid chromatography,[13,14] fluorescence spectrophotometry.[15,16] Due to the complexity of sample matrices and lower concentration of RB in lots of real samples, it is meaningful to develop an effective separation and enrichment technique to determine RB accurately.

An appropriate sample pretreatment plays important role in a whole analysis procedure due to low concentration of analytes and complicated matrix in real samples. Solid-phase extraction (SPE) as a useful technique for rapid and selective sample preparation by adsorption on a solid adsorbent has been well developed. Due to its advantages of simple operation, low cost and high enrichment, more and more adsorbents have been developed and widely applied to solve many practical problems.[17–19] Recently, magnetic solid-phase extraction (MSPE) has attracted increasing interest owing to its rapid separation process and excellent adsorption efficiency.[20–22] It's a technique that uses a magnetic or magnetizable material as absorbent matrix. For MSPE procedures, fast phase separation can be achieved by using a magnet, which greatly simplifies the SPE procedure. The core part of MSPE technique lies at the adsorbent materials, which determine the selectivity and sensitivity of the method to some extent.

In recent years, graphene oxide (GO) and GO composite are popular in adsorption research because of its excellent properties,[23,24] such as high specific surface area, abundant π electrons, exceptional mechanical and thermal properties. GO is a layered material bearing abundant of oxygenous groups on their basal planes and edges, which makes it easy to be assembled onto some substrate surfaces. Thus, the negatively charged GO tends to interact with positively charged species such as heavy metal ions and dyes.[14,25,26] In addition, based on the presence of benzene rings in RB, there existed π–π interactions between GO and RB. So, for RB extraction, GO and GO

[a]School of Pharmacy, Liaocheng University, Liaocheng, Shandong 252059, China
[b]School of Pharmaceutical Sciences, Shandong University, Jinan, Shandong 250012, China. E-mail: hmliu@sdu.edu.cn; Fax: +86-931-8277088; Tel: +86-931-4968877
[c]Key Laboratory of Chemistry of Northwestern Plant Resources, Key Laboratory for Natural Medicine of Gansu Province, Lanzhou Institute of Chemical Physics, Chinese Academy of Sciences, Lanzhou 730000, China. E-mail: hdqiu@licp.cas.cn

composite have the potential to be excellent adsorbent materials.

Magnetic GO composites are commonly formed through the adsorption interaction between magnetic Fe_3O_4 nanoparticles (Fe_3O_4 NPs) and GO, which is not stable.[27] In order to increase the stability of Fe_3O_4@GO, we proposed chitosan (CS) as modification molecular coated on the surface of Fe_3O_4 NPs. CS, as a polymer, was characterized as low cost, non-toxicity, high adhesion, good adsorption properties, and easy chemical modification.[28] The positive electricity and the presence of $-NH_2$ in CS molecule induce Fe_3O_4@CS to be stable on the surface of GO substrate. Moreover, CS can further enhance the extraction efficiency of magnetic GO for RB extraction.

Coinage metals (Au, Ag), due to their "noble" characteristics with respect to their relativistic effect and relevance in chemistry, have attracted great attention in recent years.[29,30] Relativistic effect brings s–d hybridization, which accelerates the mobilization of their electrons and facilitates the formation of chemical bond. Besides, Ag and Au nanoparticles (NPs) possess many special properties such as long-term stability, a high surface-to-volume ratio, an ease of chemical modification by organic molecules containing sulfhydryl (–SH), and so on. Taking advantage of these characteristics, Au and Ag NPs have been widely used in sample preconcentration and separation science.[31–33] And we have successfully synthesized a novel magnetic graphene oxide modified with Au nanoparticles. The magnetic composite was successfully developed as MSPE adsorbents for the determination of trace RB coupled with fluorescence technique achieving satisfactory results.[33] The presence of electron transference between RB (π-donor system) and the valency shell of Au can strengthen the affinity, thus the extraction capacity of RB can be improved.[30,33] In view of the similar properties of Ag with Au and that Ag has lower costs, Ag NPs modified magnetic graphene oxide was prepared in this paper.

Based on the above considerations, in this study, we prepared a novel magnetic composite (Fe_3O_4@CS/GO/Ag) modified with chitosan (CS), graphene oxide (GO) and Ag nanoparticles (Ag NPs). By combining the MSPE technique with fluorescence detection, the prepared Fe_3O_4@CS/GO/Ag was applied for the determination of RB in aqueous solution. Under the optimal conditions, the proposed method was successfully applied for the determination of RB in waste water, soft drink, shampoo and red pencil samples.

2 Experimental

2.1 Chemicals and instruments

Fe_3O_4 NPs (30 nm), trimethoxysilylpropanethiol and CS were obtained from Aladdin Chemical Reagent Co. Ltd. (Shanghai, China). GO (thickness: 0.55–1.2 nm, width: 0.5–3 μm) was purchased from Nanoon Nanomaterials Science and Technology Co., Ltd. (Beijing, China). Silver nitrate ($AgNO_3$), trisodium citrate, RB and sodium chloride (NaCl) were all purchased from Sinopharm Chemical Reagent Co. Ltd. (Shanghai, China). Hydrochloric acid (HCl), sodium hydroxide (NaOH), ethanol, methanol, acetonitrile, acetone, *n*-hexane and chloroform were all purchased from Beijing Chemical Factory (Beijing, China).

An F-4600 fluorescence spectrophotometer (Hitachi, Japan) equipped with 1 × 1 cm quartz cell and a xenon lamp was used for fluorescence analysis. Spectra measurement were carried out on fluorescence scan mode with the slit widths of 10 nm and the excitation and emission wavelengths of 540 and 575 nm, respectively. The PMT detector was set on 700 V for recording the emission lines. The as-prepared adsorbent was dried in the vacuum oven purchased from Shanghai Yiheng Science Instrument Co. Ltd. (Shanghai, China). An S-4800 field emission scanning electron microscope (Hitachi, Japan) equipped with an energy dispersive X-ray spectroscopy (EDS) was used for investigating the surface characteristics and frameworks of the prepared adsorbents. A vibrating sample magnetometer (VSM, VersaLab, Quantum Design, USA) was used for testing the magnetic properties of the prepared adsorbents at room temperature with a magnetic field from 30 to −30 KOe. A thermostatic oscillator (SHA-B) purchased from Changzhou Zhiborui instrument manufacturing co. Ltd. (Changzhou, China) was used for accelerating the adsorption and desorption process.

2.2 Preparation of Fe_3O_4@CS/GO/Ag

2.2.1 Preparation of Fe_3O_4@CS. The preparation process of the CS functionalized magnetic nanoparticles (Fe_3O_4@CS) applied a procedure as reported earlier to our previous work.[33–35] Briefly, chitosan (0.3 g) was firstly dissolved in 50 mL acetic acid solution (1%, v/v) under mechanical stirring. Then Fe_3O_4 NPs (2.0 g) was the added to chitosan solution. After vigorously stirring for 30 min, 50 mL of 1 M NaOH solution was added to the suspension to precipitate the Fe_3O_4@CS nanoparticles. Finally, the obtained Fe_3O_4@CS nanoparticles were washed with deionized water until the pH reached 7.0.

2.2.2 Preparation of Fe_3O_4@CS/GO. The synthesis of Fe_3O_4@CS/GO was referred to our previous work.[33,36] Firstly, GO (0.10 g) was added to 100 mL deionized water under ultrasonic treatment until GO achieving well dispersion. Then, the Fe_3O_4@CS (2.0 g) were added to GO aqueous solution (1 mg mL^{-1}) and stirred at 80 °C for 12 h for the bonding of GO. Finally, the prepared Fe_3O_4@CS/GO was washed with deionized water and methanol then dried under vacuum for 24 h at 60 °C.

2.2.3 Preparation of Ag NPs gel. $AgNO_3$ (0.047 g) was dissolved in 140 mL distilled water, then, $AgNO_3$ aqueous solution was added into a round-bottom flask and then heated at 120 °C under vigorous stirring. When the system was boiling, 10 mL of trisodium citrate aqueous solution (1%, w/w) was added quickly. The solution turned to brown in 10 min and the Ag NPs were produced. The system was kept at 120 °C for 1 hour continuously and then cooled to room temperature. The prepared Ag NPs gel was stored at room temperature and needed to be kept away from light.[32]

2.2.4 Preparation of Fe_3O_4@CS/GO/Ag. Based on the presence of lots of hydroxyl and carboxyl groups on the surface of graphene oxide and lots of hydroxyl groups in chitosan, the trimethoxysilylpropanethiol was anchored to both the GO and

the CS *via* C–O–Si bonding referred to the previous work.[33,37] Firstly, the prepared Fe_3O_4@CS/GO was suspended in dry toluene (80 mL) and then trimethoxysilylpropanethiol (1 mL) was added. The suspension was stirred and refluxed for 48 h. Then the resultant sulfydryl-modified Fe_3O_4@CS/GO was washed with toluene, ethanol, and deionized water and dried under vacuum for 12 h at 60 °C. Based on the attraction between Ag NPs and –SH, Fe_3O_4@CS/GO/Ag was also prepared referred to the previous work.[32,36] The dried sulfydryl-modified Fe_3O_4@CS/GO was added to Ag NPs sol (100 mL) under stirring for 3 h for the adsorption of Ag NPs. Finally, the prepared Fe_3O_4@CS/GO/Ag was dried under vacuum at 60 °C. The whole preparation process of Fe_3O_4@CS/GO/Ag was shown in Fig. 1.

2.3 Samples collection and preparation

2.3.1 Preparation of the RB stock solution and working solution. Stock solution of the RB (1.0 mg mL^{-1}) was prepared with ultrapure water and stored at 4 °C in darkness. In the optimization process of extraction and desorption parameters, working solution (1 μg L^{-1}) was obtained by diluting the stock solutions with ultrapure water. When measuring the linear range, all the different standard solutions (0.1, 0.2, 0.3, 0.4, 0.5, 0.8, 1.0, 1.5, 2.0, 2.5, 3.0, 3.5, 4.0, 4.5, 5.0, 5.5, 6.0, 6.5, 7.0 μg L^{-1}) were also prepared by diluting the stock solutions in this work. The pH of all the working solution is adjusted using HCl and NaOH.

2.3.2 Real samples preparation. Appropriate amounts of soft drink, shampoo and pencil samples were obtained from the local markets. The wastewater sample was obtained from local industry. The samples were prepared as follows:

Soft drink and waste water. They were filtered through 0.45 μm cellulose membrane filter (Millipore) and adjusted to 6.0 using HCl/NaOH.

Shampoo. An amount of 1.0 g shampoo was accurately weighed and then dissolved in ultrapure water and diluted to 50 mL in a volumetric flask. Then 0.5 mL of the solution was further diluted to 50 mL with ultrapure water in a volumetric flask and adjusted to 6.0 using HCl/NaOH.

Pencil. An amount of 20 mg red pencil lead was accurately weighed. Then it was dissolved in ultrapure water and filtered subsequently. The filtrate was diluted to 50 mL in a volumetric flask. Then 0.05 mL of the solution was diluted to 50 mL with ultrapure water and adjusted to 6.0 using HCl/NaOH.

All these prepared sample solutions were stored at 4 °C in darkness for further extraction and analysis of RB.

2.4 MSPE procedure

The diagram of MSPE process was shown in Fig. 2. Firstly, Fe_3O_4@CS/GO/Ag (5 mg) was dispersed into the RB standard or sample solutions (50 mL). Then the mixture was placed on a thermostatic oscillator and allowed to equilibrate for 20 min at 40 °C. Afterwards, the Fe_3O_4@CS/GO/Ag with RB adsorbed was separated from the solution by using an external magnet. Finally, the isolated Fe_3O_4@CS/GO/Ag was eluted with ethanol (3.0 mL) for desorption of the earlier adsorbed RB. In the MSPE procedure, an optimal rotating speed (150 rpm) was used to accelerate the extraction and desorption process.

3 Results and discussion

3.1 Characterization of the adsorbents

The surface structure and properties of the adsorbents were investigated by an S-4800 field emission scanning electron microscope. The SEM images of Fe_3O_4 (Fig. 3A), Fe_3O_4@CS (Fig. 3B), Fe_3O_4@CS/GO (Fig. 3C) and Fe_3O_4@CS/GO/Ag (Fig. 3D) were shown in Fig. 3. As shown in Fig. 3A and B, their surface morphologies were very similar, which demonstrated that CS was evenly covered on the surface of Fe_3O_4. As shown in Fig. 3C, it revealed that Fe_3O_4@CS NPs have successfully modified onto the surface of GO. From Fig. 3D, it can be observed that more nanoparticles distributed on the surface of Fe_3O_4@CS/GO. It can be preliminarily indicated that Ag NPs have been modified to the surface of Fe_3O_4@CS/GO.

To further illustrate the successful modification of Ag NPs to the surface of Fe_3O_4@CS/GO, the elementary composition of Fe_3O_4@CS/GO/Ag was studied in the work by EDS. EDS results

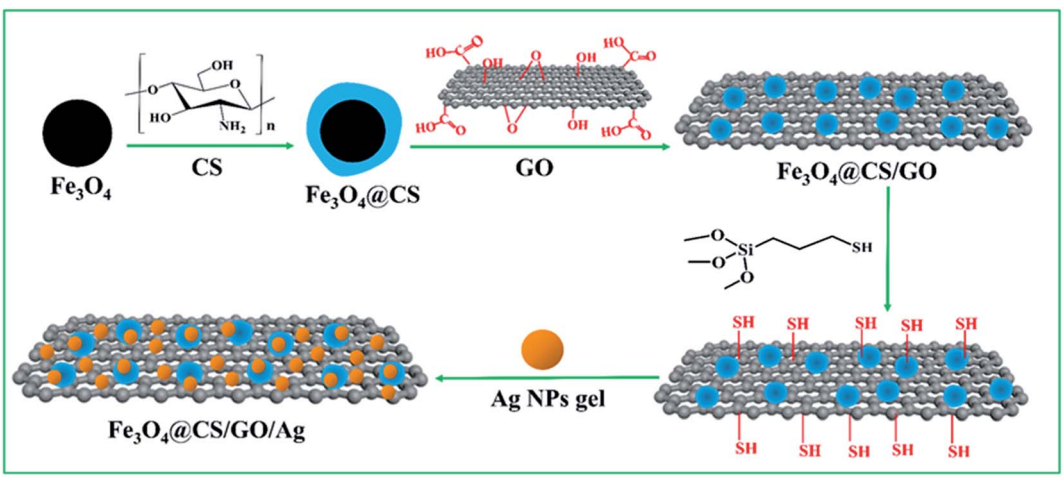

Fig. 1 The preparation process of Fe_3O_4@CS/GO/Ag.

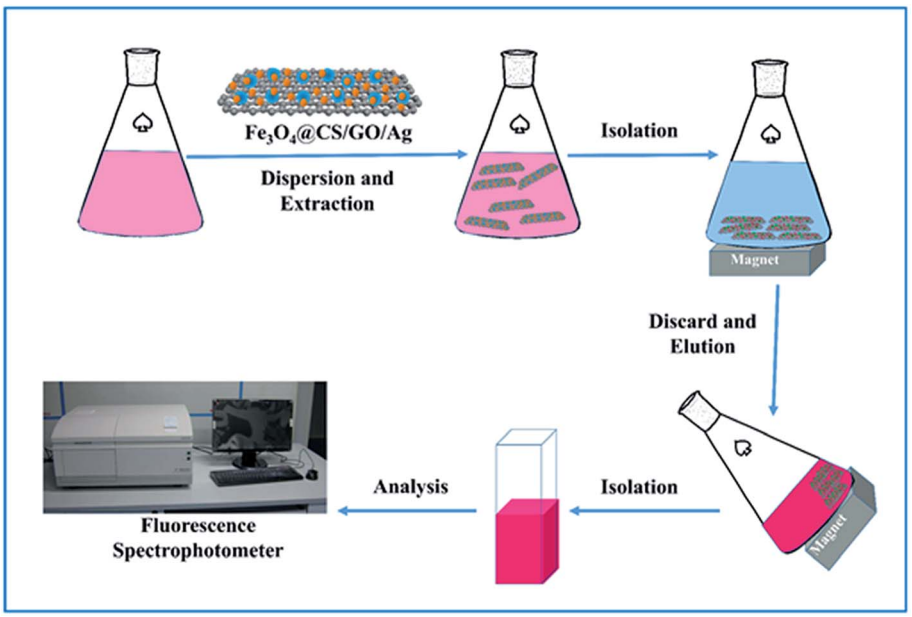

Fig. 2 The MSPE process and fluorescence analysis of RB.

were shown in Fig. 4. As shown in Fig. 4A and B, Fe, Ag, silicon, sulfur *etc.* were detected on the surface of Fe_3O_4@CS/GO/Ag, which certified that the successful preparation of Fe_3O_4@CS/GO/Ag. In addition, as shown in Fig. 4A, we can see that all the elements achieved uniform distribution on the surface of the magnetic adsorbent. Meanwhile, the percentage of each element is 2% C, 1% N, 25% O, 5% Si, 5% S, 54% Fe and 8% Ag, respectively.

The magnetic properties of Fe_3O_4, Fe_3O_4@CS, Fe_3O_4@CS/GO and Fe_3O_4@CS/GO/Ag were studied by VSM at room

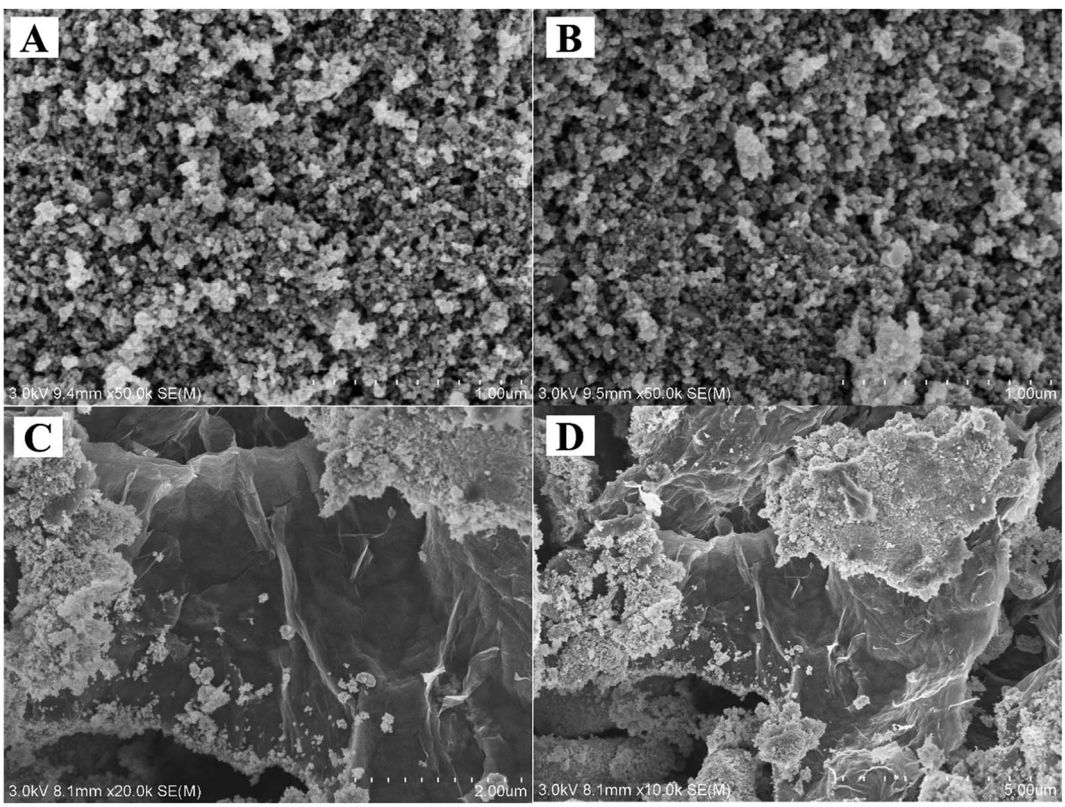

Fig. 3 The SEM images of Fe_3O_4 (A), Fe_3O_4@CS (B), Fe_3O_4@CS/GO (C) and Fe_3O_4@CS/GO/Ag (D).

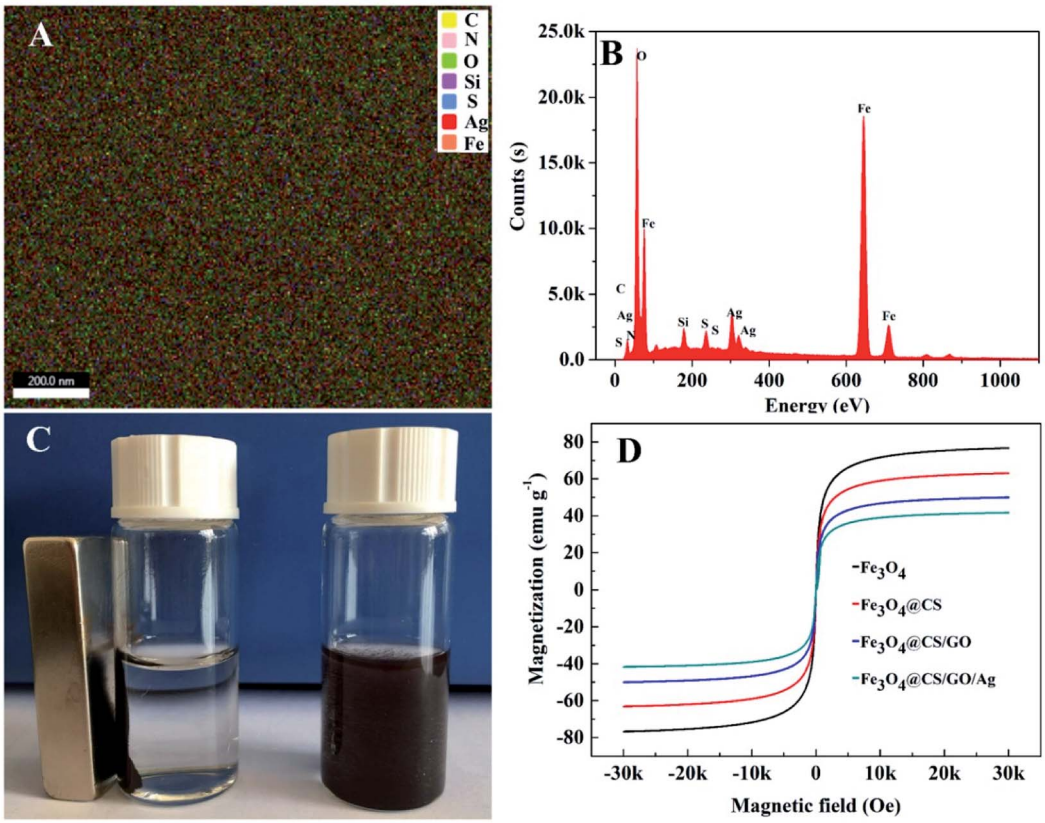

Fig. 4 The EDS image (A) and element analysis (B) of Fe_3O_4@CS/GO/Ag. The MSPE illustration (C) and the saturation magnetization of Fe_3O_4, Fe_3O_4@CS, Fe_3O_4@CS/GO and Fe_3O_4@CS/GO/Ag at room temperature (D).

temperature. As shown in Fig. 4D, the saturation magnetization (M_s) of Fe_3O_4 was 76.8 emu g^{-1}, and the M_s decreased to 63.2 emu g^{-1}, 50.0 emu g^{-1} and 41.8 emu g^{-1} after the modification of CS, GO and Ag NPs, respectively. From Fig. 4C, although the saturation magnetization value became lower than that of Fe_3O_4, it stilled enough to meet rapid separation from its water dispersion by an external magnet within 30 s.

3.2 Optimization of extraction and desorption parameters

For guaranteeing high extraction efficiency, the following primary extraction parameters (ionic strength, temperature, time, pH, adsorbent amount and oscillation frequency) and desorption parameters (type of eluent, volume of eluent and elution time) were all studied in this work. All the optimization results were shown in Fig. 5. In the work, two rounds of optimization experiments were carried out in the process of optimization. In the first round of optimization process, we optimized the parameters one by one. And then we optimized it as described in Fig. 5. When investigating one parameter, the others were all at optimal conditions that were initially obtained from the first round of optimization process.

3.2.1 Investigation of extraction parameters (ionic strength, pH, time, temperature, adsorbent amount and oscillation frequency). Ionic strength usually has a great effect on the extraction ability. Fig. 5A showed the NaCl concentration *versus* fluorescence intensity (FL intensity) relationship for RB. We can see that FL intensity of RB increased as the salt content increasing from 0 to 30 wt%. So, the salting-out effect played the major role. Because a 30% NaCl content was close to the saturated concentration in water at room temperature. Thus, further experiments were performed with the addition of 30% NaCl concentration.

In the whole extraction process, pH of working media was one of critical parameters for partitioning the analytes especially those bearing ionizable polar groups. The effect of solution pH on the adsorption of RB was presented in Fig. 5B. From pH 4.0 to pH 6.0, the FL intensity of RB was increasing. RB adsorption reached peak-point at pH 6.0, and subsequently decreased at higher pH. The carboxylic group of RB ($pK_a = 3$) becomes deprotonated at pH > 3.[15] After deprotonation, the negative electricity leaded to the lowered electrostatic attraction between RB and GO. However, negatively charged RB can lead to better π–π interactions between GO and RB. Also, it can lead to better attraction (electrostatic interaction and electron transference) between Ag NPs and RB. Hence, with pH increased from pH 4.0 to pH 6.0, RB adsorption improved due to the enhanced electrostatic interaction between RB and adsorbent. However, with pH > 6, the negative electricity of adsorbent increased which led to the lowered electrostatic attraction between adsorbent and negatively charged RB. Consequently, pH 6.0 was selected as the optimal value.

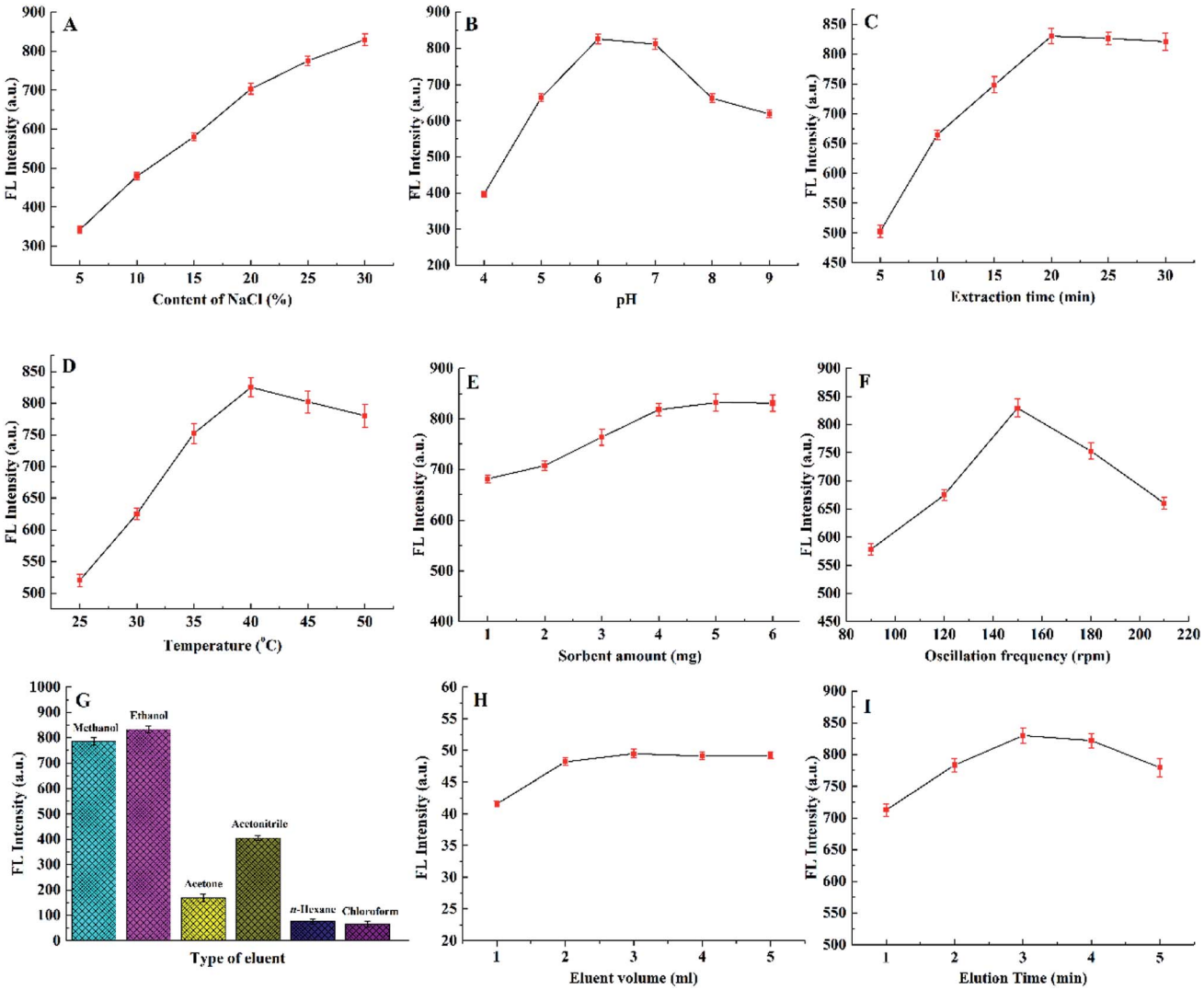

Fig. 5 Effects of extraction conditions (ionic strength, pH, time, temperature, adsorbent amount and oscillation frequency) and desorption conditions (types of eluent, volume of eluent and elution time) with RB concentration 1 μg L^{-1} and volume 50 mL.

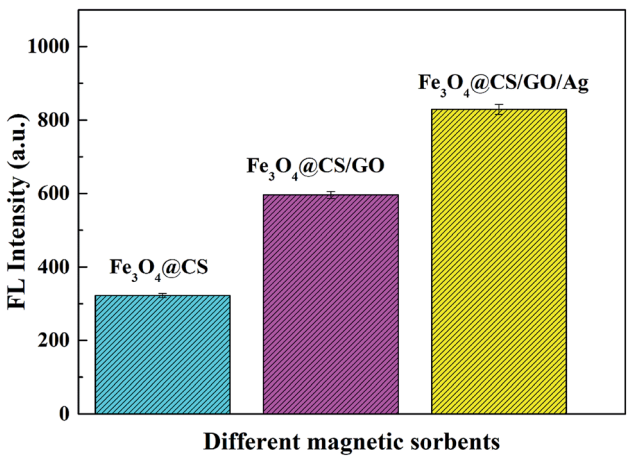

Fig. 6 Comparison of extraction efficiencies among Fe_3O_4@CS, Fe_3O_4@CS/GO and Fe_3O_4@CS/GO/Ag with RB concentration 1 μg L^{-1} and volume 50 mL.

The extraction time was defined as the time interval which was decided on the adsorption equilibrium of analytes between the adsorbent and sample solution. In our study, to evaluate the effect of extraction time, the extraction time was investigated from 5 to 30 min. As shown in Fig. 5C, the FL intensity for RB gradually increased up from 5 to 20 min. Further increasing of extraction time (longer than 20 min) can't improve obviously the extraction efficiency. Therefore, the optimum extraction time was set at 20 min, which could meet the need of rapid analysis.

Generally speaking, the extraction temperature also plays an important role in the whole extraction process. On the one hand, an elevated temperature can accelerate the mobility of the molecules and improve extraction rate; on the other hand, the analytes may be desorbed from the adsorbent by exothermic extraction at higher temperatures. Fig. 5D showed the extraction temperature *versus* FL intensity relationship for RB. 40 °C was chosen as the optimal extraction temperature for the extraction of analytes.

Table 1 Comparison of the results of the developed method with other methods

Method	Adsorbent	LR[a] (μg L^{-1})	LOD[b] (μg L^{-1})	RSD[c] (%)	Reference
MSPE-fluorescence	Fe_3O_4@CS/GO/Ag	0.2–6.0	0.05	<3.0	This method
MSPE-fluorescence	Fe_3O_4/ANI-NA (50–50)	0.35–5.00	0.10	2.10–8.20	15
MSPE-fluorescence	Fe_3O_4@SiO_2@IL MNPs	0.4–140.0	0.06	0.45	16
MSPE-fluorescence	Fe_3O_4@CS/GO/Au	0.1–6.0	0.03	<3.0	33
MSPE-HPLC-UV-visible	Fe_3O_4@MIPs NPs	100–8000	3.4	<2	7
MSPE-HPLC-DAD	Fe_3O_4@SiO_2@[OMIM]PF_6	0.5–150.0	0.08	0.51	13

[a] Linear range. [b] Limit of detection. [c] Relative standard deviation.

To evaluate the influence of adsorbent amount on extraction efficiency, different amounts of Fe_3O_4@CS/GO/Ag powder were investigated. Fig. 5E showed the extraction efficiency increased when the adsorbent amount varied form 1 mg to 5 mg, then achieved the maximum and kept invariant in the range of 5–6 mg. Based on the analysis, 5 mg was the optimal amount of adsorbent for the subsequent extraction analysis.

Oscillation can accelerate the mobility of RB molecules from the solution to the adsorbent surface and then improve the extraction efficiency. As shown in Fig. 5F, the FL intensity for RB increased with the oscillation frequency up to 150 rpm. Further increasing of oscillation frequency made the extraction efficiency of RB decreased obviously. Because when the oscillation frequency was higher than 150 rpm, it caused bubble formation which can block the transfer of RB molecules. Hence, 150 rpm was selected as the optimal oscillation frequency.

3.2.2 Investigation of desorption parameters (type of eluent, volume of eluent and elution time). In the desorption process, the choice of eluent was particularly important. In this study, six kinds of organic solvents, namely methanol, ethanol, acetonitrile, acetone, *n*-hexane and chloroform, were evaluated for their desorption efficiencies. As shown in Fig. 5G, the results showed the order of desorption ability was ethanol > methanol > acetonitrile > acetone > *n*-hexane > chloroform. The adsorbent exhibited a relatively lower degree of dispersion in chloroform and *n*-hexane, which resulted in less RB desorption. In addition, the presence of carbonyl and chlorine in acetone and chloroform could lead to the quenching of fluorescence signal. Therefore, ethanol was adopted as the optimal eluent.

For the choosing of eluent volume, it should be sufficient enough to desorb all the analytes from the adsorbent and also be as small as possible to increase the enrichment factor. To evaluate the effects of eluent volume, 1 mL, 2 mL, 3 mL, 4 mL, 5 mL, and 6 mL of ethanol were investigated. As shown in Fig. 5H, the quantitative elution (above 98.0%) was obtained when the volume of ethanol was 3.0 mL.

Elution time also played an important role in the whole analysis process. As shown in Fig. 5I, through our exploring, a duration time of 3.0 min appeared to be best for complete desorption. A longer or shorter time was not beneficial for the elution efficiency. Therefore, 3.0 min was selected as the optimum elution time.

3.3 Comparison of different adsorbents

In this study, we compared the adsorption performances of Fe_3O_4@CS, Fe_3O_4@CS/GO and Fe_3O_4@CS/GO/Ag. All the extraction and desorption experiments were performed under the optimal conditions. From Fig. 6, the results illustrated that the extraction efficiency of Fe_3O_4@CS/GO/Ag was the best. Due to the adding of π–π interactions between GO and RB, the extraction efficiency of Fe_3O_4@CS/GO increased significantly compared with Fe_3O_4@CS. After Fe_3O_4@CS/GO was modified with Ag NPs, the extraction efficiency of Fe_3O_4@CS/GO/Ag showed a further increasing, which due to Ag NPs' excellent

Table 2 Determination results of the real samples and the recoveries for spiked samples[a]

Samples	Spiked (μg L^{-1})	Found ± SD (μg L^{-1})	Recovery, RSD (%)	Contents
Waste water	—	0.65 ± 0.01	—	0.65 μg L^{-1}
	0.5	1.13 ± 0.02	96 ± 4	
	2.0	2.62 ± 0.02	97 ± 4	
Soft drink	—	Not detected	—	Not detected
	0.5	0.49 ± 0.02	95 ± 6	
	2.0	1.92 ± 0.04	96 ± 3	
Shampoo	—	0.90 ± 0.03	—	4.5 μg g^{-1}
	0.5	1.38 ± 0.03	96 ± 5	
	2.0	2.88 ± 0.02	97 ± 3	
Pencil	—	0.75 ± 0.03	—	1.88 mg g^{-1}
	0.5	1.21 ± 0.03	94 ± 5	
	2.0	2.70 ± 0.02	96 ± 3	

[a] SD: standard deviation.

electronic mobility. Therefore, between RB and adsorbents, there existed electrostatic interaction, π–π interactions and electron transference between RB (π-donor system) and Ag (acceptor system), which rendered Fe_3O_4@CS/GO/Ag excellent extraction efficiency.[33,37]

3.4 Method validation and comparison with other methods

Under the optimum conditions, the analytical characteristics of the method, such as linearity, limit of detection (LOD) and limit of quantification (LOQ), reproducibility, were investigated. From Table 1, the proposed method exhibited wide linear ranges (0.2–6.0 μg L^{-1}) with good linearity ($R^2 = 0.9992$), LOD, defined as the concentrations at signal-to-noise ratios (S/N) of 3, was 0.05 μg L^{-1}. LOQ, on the basis of signal-to-noise ratios (S/N) of 10, was 0.2 μg L^{-1}. Before extraction, the initial volume (V_0) was 50 mL, the mass of RB in the solution was m_o and the concentration of RB was C_0 ($C_0 = m_o/V_0$). After extraction and desorption, the final volume (V_1) was 3 mL. Within the linear range, the recovery rate (R) achieved 98%, so the mass of RB in desorption solution was m_1 ($m_1 = m_o \times R$) and the concentration of RB was C_1 ($C_1 = m_1/V_1 = 98\%\ m_o/V_1$). Therefore, the enrichment factor (EF) of Fe_3O_4@CS/GO/Ag-based MSPE procedure was 16.7 $\left(\mathrm{EF} = C_1/C_0 = \frac{V_0}{V_1} \times R\right)$. In addition, the adsorbent of Fe_3O_4@CS/GO/Ag can be simply recycled and reused with the obtained relative standard deviation (RSD) was less than 3.0%. As shown in Table 1, we also compared with other methods for the extraction of RB. This method with Fe_3O_4@CS/GO/Ag based MSPE also exhibited a relatively low detection limit.

3.5 Analysis of real samples

In order to demonstrate the applicability and reliability of the proposed method, it was successfully applied for determining the content of RB in waste water, soft drink, shampoo, and red pencil samples. From the results shown in Table 2, RB was not detected from the soft drink samples while detected in waste water, shampoo, and red pencil samples. To test the accuracy of the established method, two concentrations (0.5 μg L^{-1} and 2.0 μg L^{-1}) of RB were spiked for the four real samples, respectively. The spiked samples (0.5 and 2.0 μg L^{-1}) were all prepared by adding the RB standard solution to the sample solutions prepared before extraction. As shown in Table 2, the results showed recoveries were between 94% and 97% with RSD from 3% to 6%.

4 Conclusions

For the determination of trace RB, a novel magnetic composite (Fe_3O_4@CS/GO/Ag) was successfully prepared and characterized. The adsorbent of magnetic graphene oxide modified with chitosan and Ag nanoparticles. The modification of CS, GO and Ag endowed Fe_3O_4@CS/GO/Ag with high extraction performance. Compared with the Fe_3O_4@CS/GO, the extraction efficiency of Fe_3O_4@CS/GO/Ag improved obviously. On the one hand, Ag NPs further increases the specific surface area of the adsorbent; on the other hand, it exist electron transference between RB and Ag which strengthened the affinity. In addition, the main parameters affecting extraction and desorption efficiency were all optimized systematically. Under optimum conditions, good linearity, low LOD and satisfactory spiked recoveries were achieved. The developed method as a simple and efficient extraction and preconcentration technique was successfully applied for trace analysis of RB in waste water, soft drink, shampoo, and red pencil samples, which indicated the resultant adsorbent had satisfactory practicability and operability.

Conflicts of interest

The authors declare that they have no competing interests.

Acknowledgements

We gratefully acknowledge that financial supports from the National Natural Science Foundation of China (21675071) and the Fundamental Research Funds of Shandong University (2017GN0031).

References

1 R. Jain, M. Mathur, S. Sikarwar and A. Mittal, *J. Environ. Manage.*, 2007, **85**, 956–964.
2 M. R. Longmire, M. Ogawa, Y. Hama, N. Kosaka, C. A. S. Regino and P. L. Choyke, *Bioconjugate Chem.*, 2008, **19**, 1735–1742.
3 S. Steplin Paul Selvin, A. Ganesh Kumar, L. Sarala, R. Rajaram, A. Sathiyan, J. Princy Merlin and I. Sharmila Lydia, *ACS Sustainable Chem. Eng.*, 2017, **6**, 258–267.
4 M. Rahmani, M. Kaykhaii and M. Sasani, *Spectrochim. Acta, Part A*, 2018, **188**, 164–169.
5 W. Wang, Y. Du, Z. Xiao, Y. Li, B. Li and G. Yang, *Anal. Sci.*, 2017, **33**, 715–717.
6 S. Wang, B. Yang and Y. Liu, *J. Colloid Interface Sci.*, 2017, **507**, 225–233.
7 X. M. Su, X. Y. Li, J. J. Li, M. Liu, F. H. Lei, X. C. Tan, P. F. Li and W. Q. Luo, *Food Chem.*, 2015, **171**, 292–297.
8 N. Ozkantar, M. Soylak and M. Tuzen, *Turk. J. Chem.*, 2017, **41**, 987–994.
9 Y. E. Unsal, M. Soylak and M. Tuzen, *Desalin. Water Treat.*, 2014, **55**, 2103–2108.
10 M. Soylak, Y. E. Unsal, E. Yilmaz and M. Tuzen, *Food Chem. Toxicol.*, 2011, **49**, 1796–1799.
11 C. Desiderio, C. Marra and D. S. Fanali, *Electrophoresis*, 1998, **19**, 1478–1483.
12 A. M. Lopez-Montes, A. L. Dupont, B. Desmazieres and B. Lavedrine, *Talanta*, 2013, **114**, 217–226.
13 J. P. Chen and X. S. Zhu, *Food Chem.*, 2016, **200**, 10–15.
14 H. Y. Zhai, L. Huang, Z. G. Chen, Z. H. Su, K. S. Yuan, G. H. Liang and Y. F. Pan, *Food Chem.*, 2017, **214**, 664–669.
15 H. Bagheri, R. Daliri and A. Roostaie, *Anal. Chim. Acta*, 2013, **794**, 38–46.
16 A. A. A. A. Bakheet and X. S. Zhu, *J. Chem. Sci.*, 2017, **5**, 1–7.

17 W. Q. Xia, P. L. Cui, G. N. Wang, J. Liu and J. P. Wang, *Anal. Methods*, 2018, **10**, 3001–3010.
18 A. Hatamie, M. Nassiri, M. D. Alivand and A. Bhatnagar, *Talanta*, 2018, **176**, 156–164.
19 M. Eftekhari, M. Gheibi, M. Akrami and F. Iranzad, *New J. Chem.*, 2018, **42**, 1159–1168.
20 L. Xia, L. Liu, X. Lv, F. Qu, G. Li and J. You, *J. Chromatogr. A*, 2017, **1500**, 24–31.
21 N. A. Kasa, E. Akkaya, B. T. Zaman, G. Çetin and S. Bakirdere, *Environ. Monit. Assess.*, 2018, **190**, 589–598.
22 E. O. Er, E. Akkaya, B. Ozbek and S. Bakırdere, *Microchem. J.*, 2019, **147**, 269–276.
23 Z. L. Cheng, Y. X. Li and Z. Liu, *J. Alloys Compd.*, 2017, **708**, 255–263.
24 L. Cai, N. Xu, S. Xia, Y. Wang and X. Chen, *J. Sep. Sci.*, 2017, **40**, 2925–2932.
25 X. M. Ren, Q. Y. Wu, H. A. Xu, D. D. Shao, X. L. Tan, W. Q. Shi, C. L. Chen, J. X. Li, Z. F. Chai, T. Hayat and X. K. Wang, *Environ. Sci. Technol.*, 2016, **50**, 9361–9369.
26 L. M. Cui, X. Y. Guo, Q. Wei, Y. G. Wang, L. Gao, L. G. Yan, T. Yan and B. Du, *J. Colloid Interface Sci.*, 2015, **439**, 112–120.
27 S. Mahpishanian and H. Sereshti, *J. Chromatogr. A*, 2017, **1485**, 32–43.
28 H. F. Zhang and Y. P. Shi, *Analyst*, 2012, **137**, 910–916.
29 J. Roithová and D. Schröer, *Chem. Rev.*, 2009, **253**, 666–677.
30 J. J. Feng, M. Sun, J. B. Li, X. Liu and S. X. Jiang, *Anal. Chim. Acta*, 2011, **701**, 174–180.
31 Q. X. Zhou, M. Lei, Y. L. Liu, Y. L. Wu and Y. Y. Yuan, *Talanta*, 2017, **175**, 194–199.
32 L. C. Wang, X. D. Hou, J. B. Li, S. J. Liu and Y. Guo, *J. Sep. Sci.*, 2015, **38**, 2439–2446.
33 L. L. Xu, H. B. Suo, J. L. Wang, F. X. Cheng, H. M. Liu and H. D. Qiu, *Anal. Methods*, 2019, **11**, 3837–3843.
34 H. B. Suo, L. L. Xu, C. Xu, H. Y. Chen, D. H. Yu, Z. Gao, H. Huang and Y. Hu, *Int. J. Biol. Macromol.*, 2018, **119**, 624–632.
35 H. B. Suo, L. L. Xu, C. Xu, X. Qiu, H. Y. Chen, H. Huang and Y. Hu, *ACS Sustainable Chem. Eng.*, 2019, **7**, 4486–4494.
36 H. M. Liu, Y. Guo, X. S. Wang, X. J. Liang and X. Liu, *RSC Adv.*, 2014, **4**, 37381–37388.
37 L. L. Xu, H. B. Suo, X. J. Liang, L. C. Wang, Y. Guo and S. X. Jiang, *RSC Adv.*, 2015, **5**, 41536–41543.